Afrique SCIENCE *24(6) (2024) 39 - 56*
ISSN 1813-548X, http://www.afriquescience.net

Petro-structural signature and gold mineralization relationship in the meridional sector of the Fettékro greenstone belt, Central-western Côte d'Ivoire, based on remote sensing and field investigations

Konan Roger ASSIE[1*], Kouadio Florentin TANI[1], Aristide Ghislain Beugré DAGO[1] et Koffi Alexis N'DRI[2]

[1] University Jean Lorougnon Guédé, UFR-Environnement, Département des Sciences de la Terre, Laboratoire de Géologie Appliquée, BP 150 Daloa, Côte d'Ivoire
[2] Institue National Polytechnique Felix Houphouët-Boigny, Ecole Supérieure des Mines et de Géologie, BP 1093 Yamoussoukro, Côte d'Ivoire

(Reçu le 13 Avril 2024 ; Accepté le 10 Juin 2024)

* Correspondance, courriel : *assiek@yahoo.com*

Abstract

This work aims to understand the geological framework of the mineralization and to establish the relationship between the gold deposit and the geology of the area. It is based on the use of optical and radar images and supplemented by a field campaign. The study yielded structural or linear maps of the study area, covering an area of 471.38 Km². The detailed map of fractures obtained after validation includes more than 6,500 fractures. The remote sensing tools have thus made it possible to draw up an updated structural diagram of the study area. The area is marked by intense fracturing, with the main directions being N00-N010, NE-SW (N040-N080) and N090-N120. The central and north-eastern sectors of the study area are the most interesting and correspond to the strongest geochemical anomalies in gold and lineament density over the entire study area. The structural study highlighted two shear zones, one N010-N025 sinister, the other N110-N120 dexter, within volcanic, metamorphic and plutonic formations, which are thought to be responsible for the gold mineralization of these formations. This work has enabled us to highlight the vector of mineralization in the area and the origin of the current architecture of the geological formations in the region.

Keywords : *structural, fracture, anomaly, gold mineralization, lineament, Landsat-7.*

Résumé

Signature pétro-structurale et relation avec la minéralisation en or dans la partie méridionale de la ceinture de roches vertes de Fettékro, Centre-ouest de la Côte d'Ivoire, au moyen de la télédétection et des investigations sur le terrain

Ce présent travail vise à comprendre le cadre géologique de la minéralisation et d'établir le lien entre le gisement d'or et la géologie de la zone. Il est basé sur l'utilisation d'images optiques et radar et renforcé par une campagne de terrain. Cette étude a permis de dresser des cartes structurales ou linéaires de la zone d'étude, couvrant une superficie de 471,38 Km². La carte détaillée des fractures obtenue après validation

comporte plus de 6500 fractures. Les outils de télédétection ont ainsi permis de proposer un schéma structural actualisé de la zone d'étude. La zone est marquée par une fracturation intense dont les directions principales sont N00-N010, NE-SW (N040-N080) et N090-N120. Les secteurs central et nord-est de la zone d'étude sont les plus intéressants et correspondent aux plus fortes anomalies géochimiques en or et en densité de linéaments sur l'ensemble de la zone d'étude. L'étude structurale a identifié deux zones de cisaillement, l'une N010-N025 senestre, l'autre N110-N120 dextre, au sein de formations volcaniques, métamorphiques et plutoniques qui seraient responsable de la minéralisation de ces formations. Ce travail nous a permis de mettre en évidence le vecteur de la minéralisation dans la zone et l'origine de l'architecture actuelle des formations géologiques de la région.

Mots-clés : *structurale, fracture, anomalie, minéralisation en or, linéament, Landsat-7.*

1. Introduction

Mineral exploration is the process of meticulously searching for minerals and valuable materials beneath the Earth's surface [1]. This extensive undertaking involves various techniques such as geological mapping, geochemical analysis, geophysical surveys, and drilling to identify and assess potential mineral deposits. The goal of mineral exploration is to locate economically viable resources that can be extracted for commercial purposes [2]. This field requires a deep understanding of geology, and the use of advanced technology to explore and access these valuable natural resources. The high value of gold has boosted prospecting and exploration of new deposits [3], making gold exploration one of the world's foremost specialties. In addition, fruitful research results require awareness of information related to geological mapping and mineral alteration zones, which helps pinpoint essential structural features and hydrothermal information related to ore deposits [4]. Therefore, geological structure governs the formation of a wide range of mineralization types, which can be tracked by investigating the lineaments depicting them. The high concentration of lineaments is an index of rock fracturing and shearing [5], greater structural deformation [6], and greater rock permeability or porosity [7]. In turn, these lineaments can represent traps for hydrothermal fluids flowing along faults and fractures and can promote the formation of hydrothermally altered rocks that will become a prospecting zone for mineral resources [8]. In particular, mapping structural lineaments is a complex process due to deep weathering, limited exposure of outcrops and heavy vegetation canopy, implying poor reachability of study areas during field surveys. Nevertheless, the advent of multispectral satellite imagery has enhanced prospecting conditions during mineral exploration phases, enabling rapid and inexpensive acquisition of data from a specific target without being in the vicinity [9]. Landsat-7 data are the result of multispectral remote sensing, a method of collecting and analyzing information about the Earth's surface through the use of sensors aboard the Landsat-7 satellite [10]. By capturing information across different wavelengths of light, Landsat-7 data enable the generation of multispectral images that are valuable for scientific research [10]. These data can be integrated with other geological data to provide a comprehensive understanding of the subsurface mineralization, and allow also to gain a more nuanced understanding of the area [11]. Most of West Africa's gold production is derived from Birimian formations [12]. Côte d'Ivoire has the largest portion of these formations, but few large-scale gold deposits have been mined. Although it has many highly promising zones, it nevertheless remains an under-explored or even unexplored land, perhaps for cultural rather than geological reasons. Gold mineralization has been indicated in the study region by indigenous workings in the past and other modern mining workings. However, exploration works using modern techniques began in the early 1970s [13]. Researchers prospecting the Fettékro range, discovered numerous rock occurrences [14]. They carried out chemical analysis that indicates appreciable grades of invisible gold, but were not confirmed. Some researchers conducted a soil sampling and geophysical program in the northern sector of the study region [15]. Unlike the septentrional region, the southern part of the region has been less explored. The origin of the gold deposits in this sector have been the subject of extensive

research, which has linked gold mineralization to hydrothermal fluid systems hosted by shear zones where gold occurs in quartz veins and altered rocks [16, 17]. To date, the relationship between primary gold mineralization and the geological features in this region has not been fully elucidated. The aim of this study is to extract regional lineaments using multispectral imaging and integrate with field investigation data to establish an understanding between geological features, and the spatial distribution and orientation of gold concentration. Fulfilling this objective may help to gain a better understanding of the gold mineralization in the region, the geological structure of the area, and assess the viability of mineral exploration in the region.

2. Methodology

2-1. Study site

2-1-1. Location of the study area

The study site is located in central-western Côte d'Ivoire between longitude 5° 10' and 5° 40' W and latitudes 6° 10' and 6° 40' N ***(Figure 1)***, in the district of Gôh-Djiboua, more precisely in the department of Oumé, between the cities of Hiré, Oumé and Kokumbo ***(Figure 2)***. It is located 250 km from the city of Abidjan, to which it is linked by a tarmac road, and covers an area of around 2,873 km².

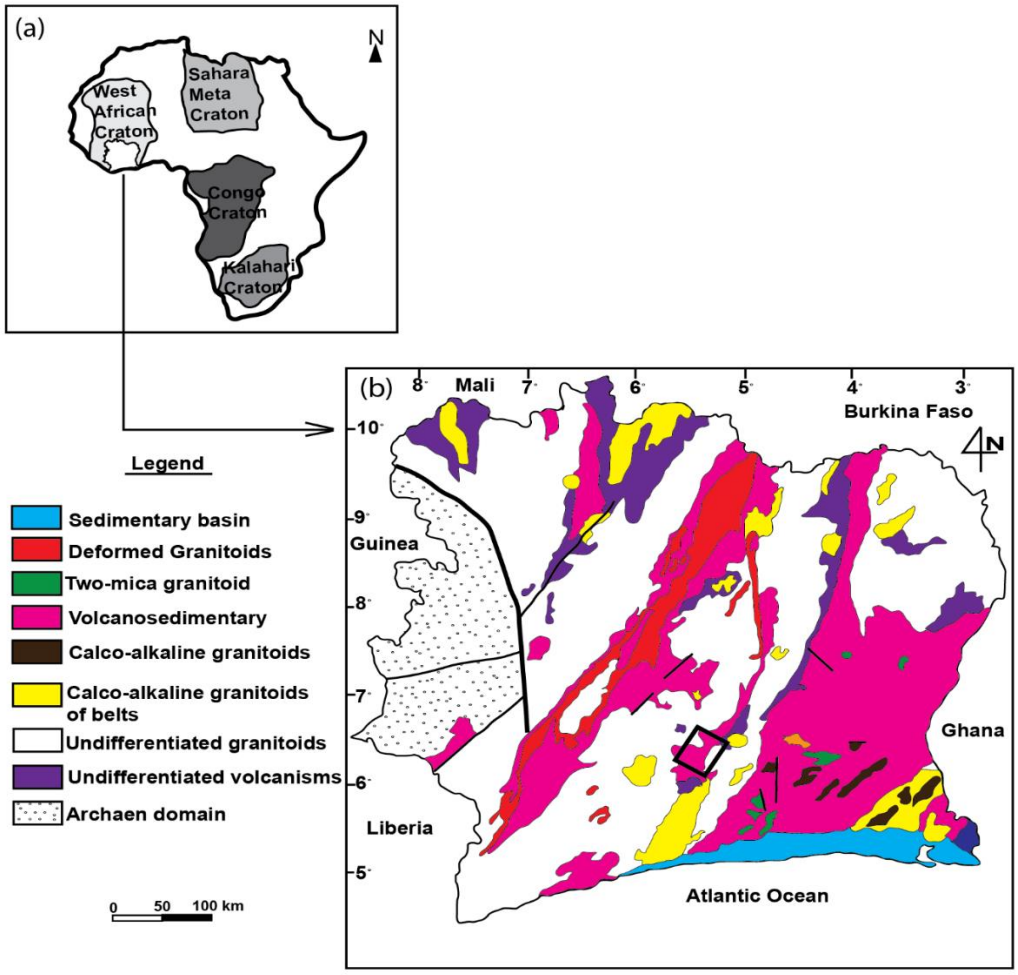

Figure 1 : *Geological context maps of the study. a. Map showing African Cratons, geological map of Côte d'Ivoire, the black square denotes the study region*

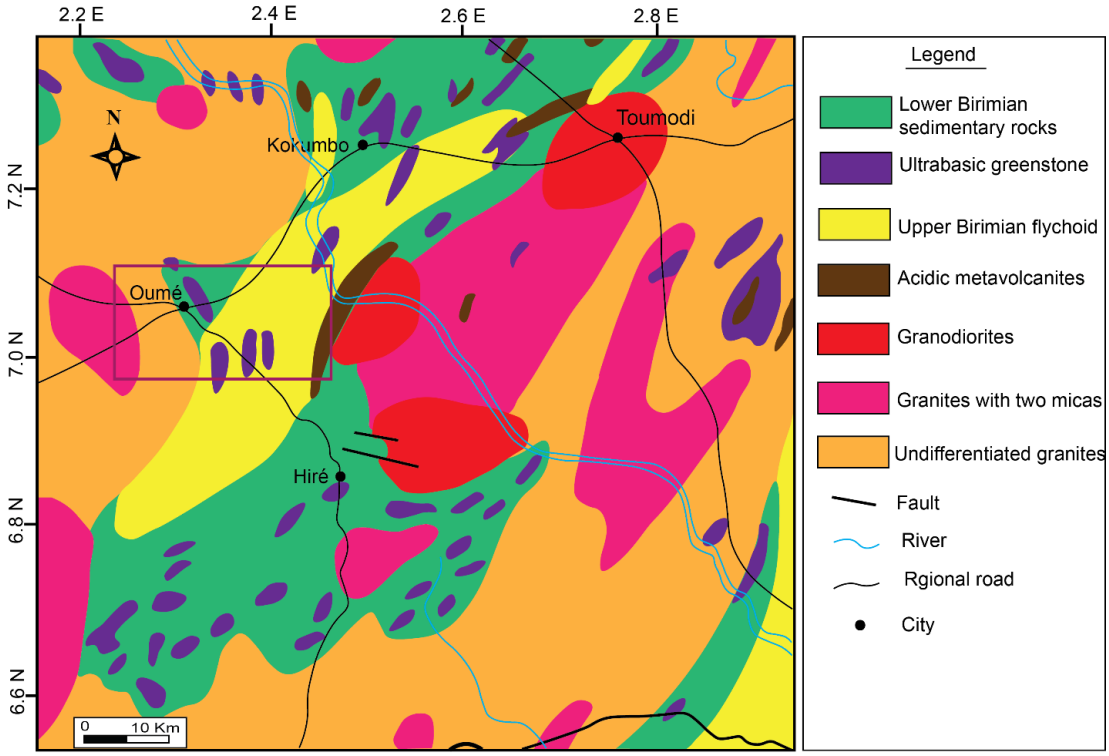

Figure 2 : *Geological map of the study region, with location of the study area (Square)*

2-1-2. Regional and local geological framework

Côte d'Ivoire lies on the Man Dorsal, southern part of the West African craton characterized by a basement of Precambrian age and a relatively recent sedimentary basin covering a third of its surface area in the extreme southern part ***(Figure 1)***. The basement is segmented into the Archean to the west and the Proterozoic domains to the east, separated by the submeridian Sassandra transcurrent fault [18]. Deformation along this shear zone is marked by transgressive, senester high-temperature structures of principal north-south extension, and continues with the same shearing regime under decreasing temperatures, resulting in mylonites and even ultramylonites at the heart of the zone [19]. The Sassandra fault is also staked by granitoid plutons ranging in age from 2.09Ga to 2.07Ga [18]. This fault is thought to be extended to the north by the Zed Ness fault in Mauritania and to the south by the Guri fault in Venezuela, South America [20]. The study area extends over the southern part of the Fettékro greenstone belt located in the central of the country, covering about 45 km of the Lower Proterozoic Birimian Supergroup ***(Figure 2)***. The area is thought to have experienced a single phase of progressive deformation at around 2.1 Ga, characterized by rugged fractures, tight north-northeast trending folds and greenschist facies metamorphism [21]. The area is predominantly underlain by volcanic rocks, chiefly basalts with some less calcareous rocks. Other rock types include felsic intrusions such as granodiorites and quartzite diorites, metasediments and various sedimentary stratigraphies composed of black shales and fine sandstones. The western margin of the permit is bounded by post-Birimian granitoids. All these different geological units can be subdivided into two major groups [22]: the group of volcano-sedimentary formations and the granitoid group. The volcano-sedimentary group includes metasediments such as metaarenites, flyschoid-trending metaargilites and metasiltites, which often overlie the metaarenites; and metavolcanites consisting of metabasalts, amphibolites, andesites, tuffs, spilites and conglomerates with metagrauwackes. We also have chloritoschists, sericite schists and undifferentiated schists. While the granitoid group comprises granitoid intrusions among these volcano-sedimentary formations and a granitic complex outcropping at the far eastern end of Doka city.

2-2. Fieldwork and sampling

The survey was carried out on fifteen rock exposures in the study area, recording the locations of structures associated with gold mineralization using a Garmin 64s portable global positioning system. During fieldwork, the rocks exhibited a variety of outcrop shapes, such as slabs, domes and boulders, and some rocks showed zones of alteration. Detailed structural work, consisting of outcrop measurements, focused on fractures, foliation and schistosity. Geological deformations were also identified and described in the study area, and the surrounding terrain and a few rock samples were taken from typical outcrops to make thin and polished sections. In addition, the thin and polished sections were described with the aid of an optical microscope in transmitted and reflected light. The study area is characterized by the scarcity of outcrops, which are highly discontinuous despite a high degree of weathering. However, the scarce outcrops are made up of schists, granites, gneisses and amphibolites, which are essentially composed of feldspars (mainly plagioclase).

2-3. Landsat-7 and radarsat-1 data

The satellite imagery covering the study area was downloaded from the United States Geological Survey (USGS) Earth Explorer website (https://earthexplorer.usgs.gov). They include the Landsat-7 ETM+ optical image (8 bands, scene 197-55) acquired on July 28, 2019, and the Radarsat-1 SAR (Synthetic Aperture Radar) image acquired on August 21, 2017. These data were then processed by various software packages, such as Envi 4.3 for georeferencing operations and satellite image processing; Mapinfo 7.5 for georeferencing maps, from which we extracted vectors representing roads and high-voltage wires, enabling us to make corrections to the imported lineamentary field produced on Envi 4. 3; LinWin and RU3 provided automatic counting and distribution of lineaments or fractures within direction classes; and finally, Surfer 7 was used to generate the lineament map expressing fracturing intensity.

2-4. Data processing

Data pre-processing phases are highly necessary to acquire radiometrically and spatially corrected images to interpret spectral data [23, 24]. Therefore, radiometric calibration was applied to Landsat-7 data to convert them into radiance data at the sensor. The aim is to extract as much structural information as possible by creating and analyzing a lineament map. The methodology is summarized in a flow chart ***(Figure 3)***. As the whole image was difficult and cumbersome, we extracted two windows for each of the images, refocused on the study area for easier processing. The study area was delimited using Envi 4.3 software, by entering the coordinates (upper left point: 225375E; 710875N and lower right point : 245325E; 700000N). Processing based on the nature of the images was carried out in several stages ***(Figure 3)***. We applied the principal component analysis method of the radiometric enhancement technique to band 2 of our optical image to highlight the structural elements.

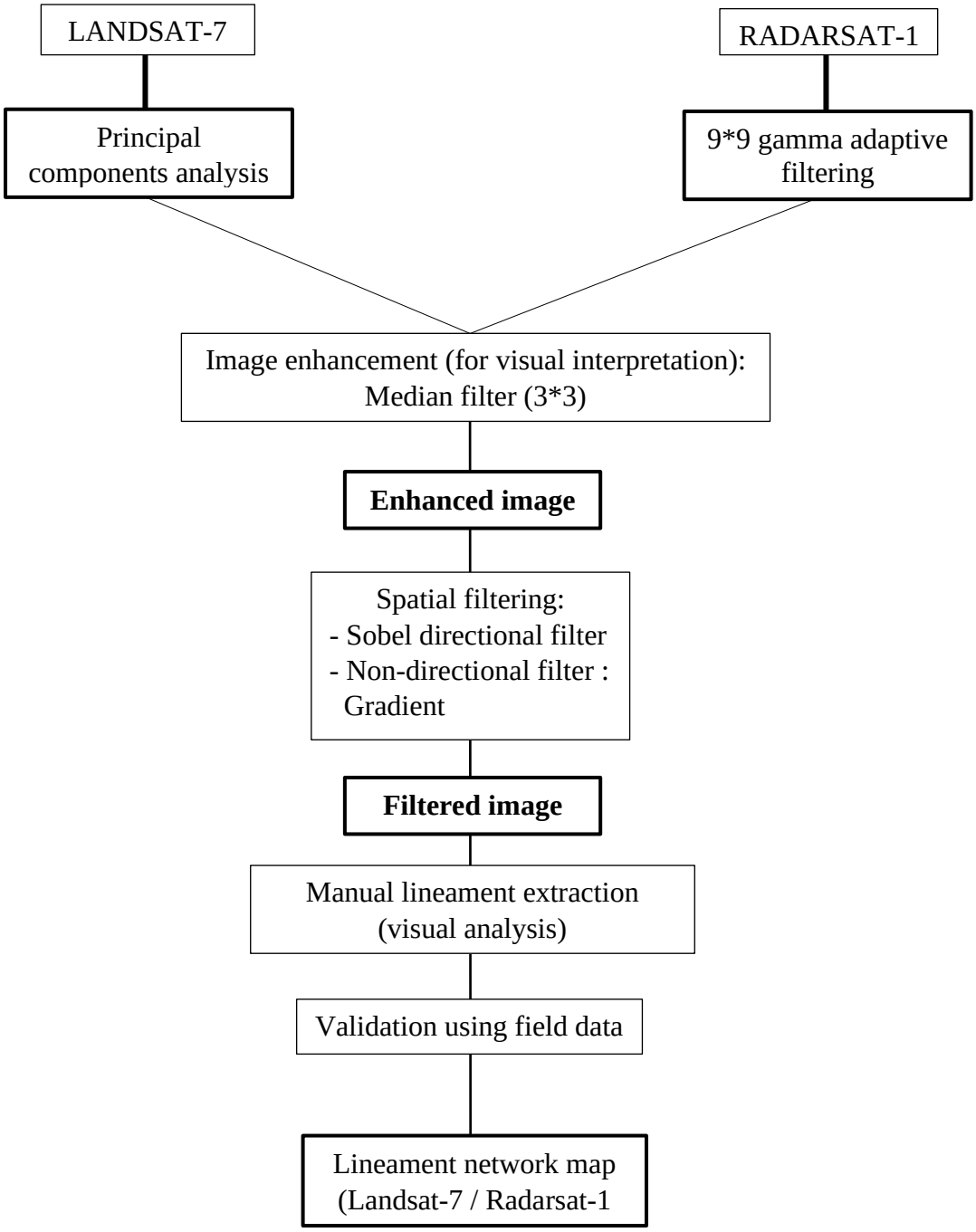

Figure 3 : *Flowchart outlining the procedure adopted in this study*

2-5. Lineament extraction from Landsat imagery

There are two methodological approaches to structural lineament mapping. The first involves automatic extraction of lineaments using mathematical morphology [7]. The second involves manual extraction of lineaments by visual analysis [25]. Image discontinuities corresponding to structural lineaments were manually extracted, following on-screen visual analysis after application of the chosen spatial filters. The same vector was used on both types of image, first optically and then with radar, in order to record the maximum number of structural elements varying from surface to depth. This operation results in the establishment of a lineament field on which to perform a geostatistical study. These lineaments were then superimposed by field data. The various structural objects interpreted are compared with existing structural data, and those obtained during fieldwork. This operation characterizes the lineaments as objects of a structural nature that can be used to interpret the major structures and morphostructures of the region.

2-6. Statistical analysis

This study involves firstly processing the lineament field using Mapinfo software, then carrying out a geometric analysis using LinWin and Surfer 7. The processing consists of eliminating all duplicated lines, triple points and isolated points, separating broken lines and readjusting lineaments. This will correct any anomalies that may have arisen when drawing the lineaments. The analysis consists in performing a statistical study of the lineaments by establishing the statistical distribution of directions, the distribution of lineament lengths and the lineament density.

3. Results

3-1. Petrographic characteristics

This study was carried out on various outcrops, from which the most representative samples of the study area were collected and analyzed. It emerged that the study area is dominated by schists such as sericite schists, chlorite schists, basalts, gabbro-quartzics and granites, and the collected representative samples encompass all these types. The sericite schists are black in color and schistose in structure ***(Figure 4a)***. Microscopic examination of the thin section ***(Figure 4b)*** shows a lepidoblastic texture, with abundant quartz, grouped in clusters within the microveins; plagioclases are small, very often associated with quartz in the microveins; sericite also forms the majority of the matrix, altered and yellowish in hue; epidote is grouped in very small size aggregates, and a bluish hue, with opaque minerals showing deformation in the direction of schistosity. The chlorite schist outcrops are black in color with a schistose structure ***(Figure 4c)***. A study of the thin section reveals a crenulation schistose texture ***(Figure 4d)***. It is composed of very abundant, large, yellowish chlorite, direct pleochroism and subdirect extinction with an extinction angle equal to 20°; quartz is abundant in the microcracks, where it forms phenoclasts; epidotes are grouped in very small aggregates; opaque minerals are also present in scarce abundance.

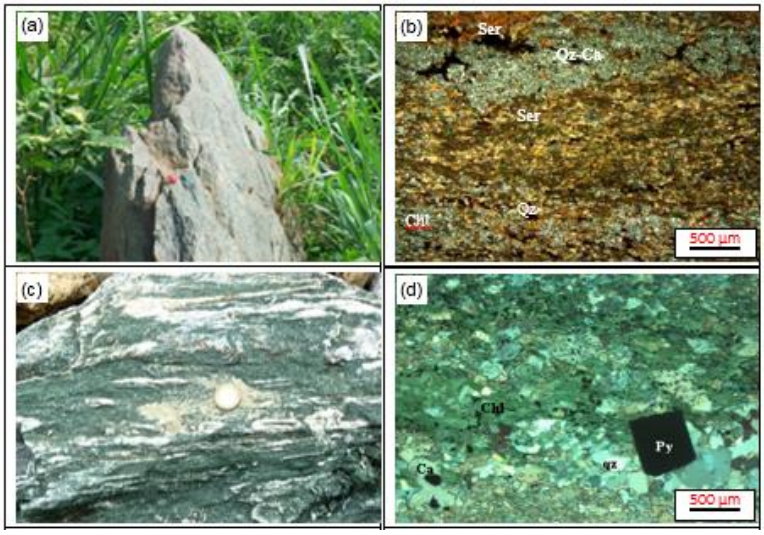

Figure 4 : *Macroscopic and microscopic photographs of rocks observed during the field investigation. a,b: sericite schists showing a greenish chlorite level between two quartz-feldspar levels with associated sericite; c,d: chlorite schists showing chlorite levels with disseminated calcite*

Metabasalts are dark-grey to green, it is marked by calcite veinlets ***(Figure 5e)***. There is also some schistosity, with disseminated sulfides (pyrite) in places. Microscopically, the texture is aphanitic, sometimes porphyritic, with fine plagioclase, chlorite and calcite ***(Figure 5f)***. They are also characterized by innumerable aggregates of fine chloritized biotite flakes and distinctly automorphic phenocrysts of clinopyroxenes fully ouralitized in secondary green hornblende. The gabbro-quartzics encountered are melanocratic granular formations. Microscopically, these formations show subautomorphic quartz, medium rock-grain size, unaltered, presence of breakage, rolling extinction; plagioclase less abundant than quartz, xenomorphic, dirty patches, some sections in the process of damouritization, medium rock-grain size or slightly larger; abundant clinopyroxene, medium rock grain size, brown but not pleochroic, altered, frequent basal sections; sericite, very abundant, makes up most of the matrix; epidote: xenomorphic, moderately cracked, with pink polarization hue, sub-right extinction relative to mineral length; and moderately abundant opaque minerals. Granite outcrops are sometimes altered, with pyrite and arsenopyrite minerals scattered throughout, while other outcrops have pyrite inclusions. They appear either as granite domes or as slabs ***(Figure 5g)***. It is sometimes silicified and intersected by quartz and sulfide veins and veinlets. Microscopic examination of the thin section shows abundant quartz, xenomorphic, in phenocrysts, with irregular fractures and remarkable rolling extinction; myrmekite is also abundant, in bud form; plagioclase are less abundant than quartz, highly altered, with medium-grain size; microcline is xenomorphic, frequent in the rock, somewhat altered; brown hornblende is less abundant than plagioclase and microcline, altered to chlorite and epidote; extinct cubic-form opaque minerals are moderately abundant ***(Figure 5h)***.

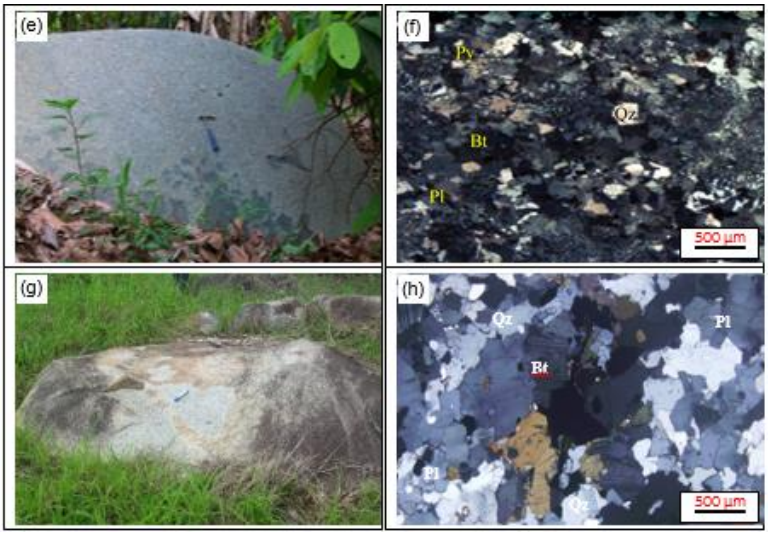

Figure 5 : *Macroscopic and microscopic photographs of rocks observed during the field investigation. e,f : metabasalt; g,h : pyrite-inclusion granite cut by quartz veins*

3-2. Structural characteristics

Structural elements of shear deformation were observed on the granite outcrop including dextral shear fractures oriented N120 and the presence of sigmoidal cracks describing the senestral shear direction ranging from N10 to N025 ***(Figure 6a)***. Granites are generally enclosed within volcanic formations. The whole is subject to brittle deformation marked by quartz veins and joints of variable direction ***(Figure 6b)***. The resulting deformation is thought to post-date the emplacement of the encountered rocks. Fracture schistosity of N170 direction was also observed on this site, affecting the metabasalt ***(Figure 6c)***. We also observe quartz-filled boudins affected by micro-fractures or fibers in N047 direction. These boudins are interconnected by a quartz vein striking N115; echelon cracks, pointing to N020 sinistral shearing ***(Figure 6a)***; N115 shear

vein indicating dextral shearing. We note also the presence of sigma type porphyroclast of k-feldspar on a mafic outcrop ***(Figure 6d)***. We observed faults ***(Figure 6e)*** of varying directions, which we were able to pinpoint to establish a chronology of the various encountered faults ***(Figure 6f)***. In chronological order, we have F1 faults running N130; F2 faults trending N170; F3 faults trending N020; F4 faults trending N180.

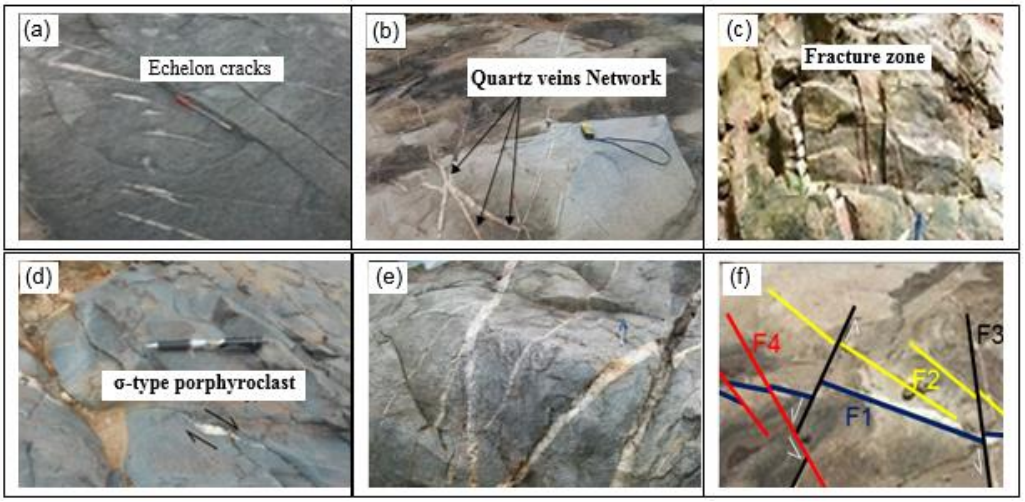

Figure 6 : *Photograph of structural features analyzed in the field. a: echelon cracks; b : Network of quartz veins. c : metabasalt affected by fracture schistosity, d : sigma type porphyroclast of k-feldspar, e : Network of quartz veins with N10-striking dextral shear fracture, f : fault chronology*

Microscopic observation of the structures of the phyllosilicate-rich and quartz-rich levels respectively, characterized by the presence of deformed sigmoidal structures describing a sinister movement ***(Figure 7a)***. This set forms an s/c fabric ***(Figure 7b)***; a quartz microvein or microscopic slit parallel to the schistosity direction, with a sigmoidal shape indicating the dextral shear direction ***(Figure 7d)***; a qurtz rubbon subparallel to the schistosity in the sericite schist are also observed ***(Figure 7c)***. The measurements carried out have enabled us to establish the directional rosette, which allows us to distinguish a class of dominant directions N050- N090 and two classes of secondary directions N00- N010 and N100- N120 ***(Figure 7e)***.

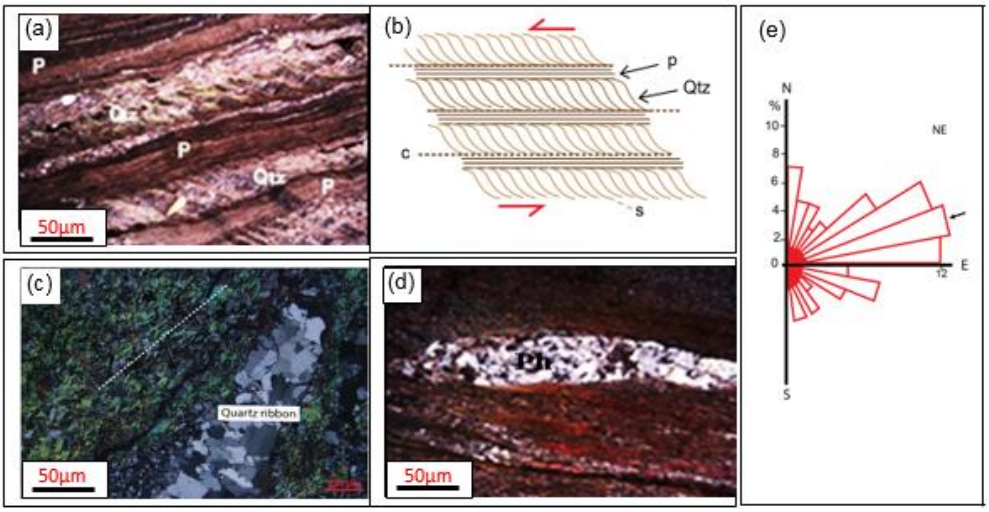

Figure 7 : *Microstructures observed on analyzed rock samples. a, b : Illustration of s/c fabric and their relationship to shear direction; c : Qurtz rubbon subparallel to the shistosity; d : Boudiné quartz phenoclast showing dextral motion (P : Phyllite, Ph : Phenoclast, Qtz : Quartz)*

3-3. Linear map analysis

3-3-1. Detailed lineaments network

We proceeded to record all discontinuities on all processed images. Roads and high-voltage lines were excluded by creating a vector different from the lineament vector. A detailed lineament map was drawn up ***(Figure 8)*** after filtering the satellite images and extracting the lineaments. This was performed over a surface area of roughly 216.96 Km², i.e. 46 % of the study zone.

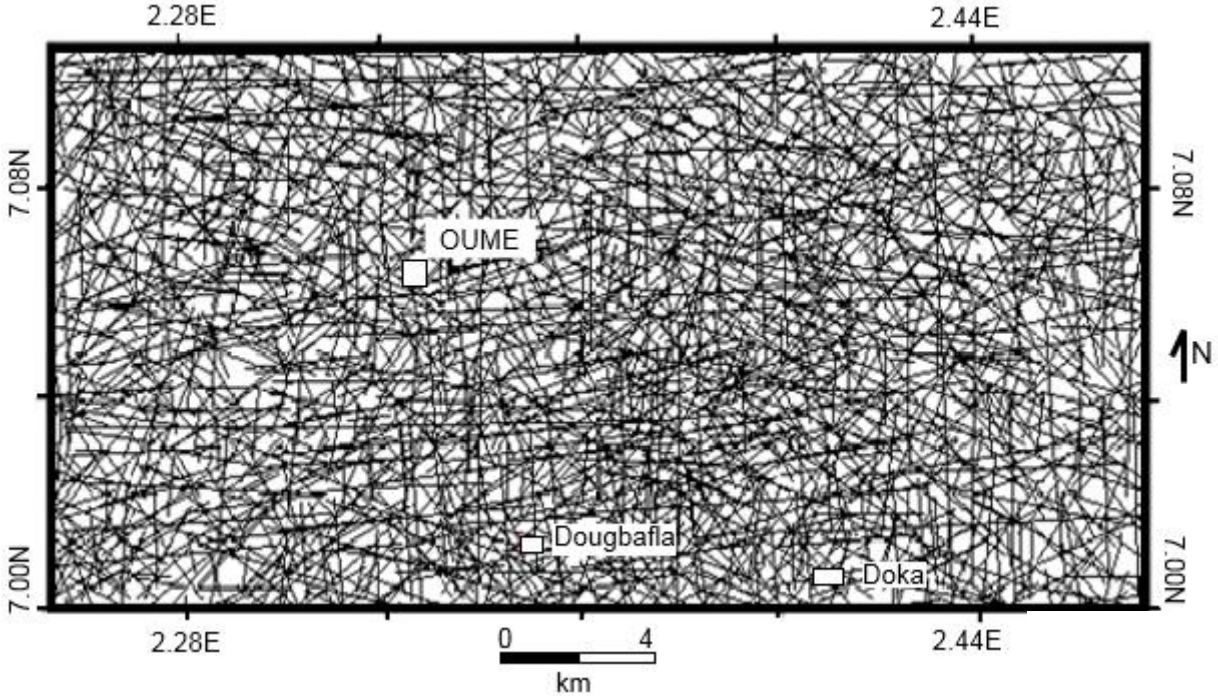

Figure 8 : *Detailed lineament map*

3-3-2. Statistical analysis of lineaments

Statistical analysis of the lineament pattern over the study area yields histograms and directional rosettes displaying the distribution of lineaments according to the encountered directions, based on the number and cumulative length of lineaments. Regard to the general orientation according to the number of lineament, the results reveal 6,345 lineaments, the most frequently observed directions in the area have been identified ***(Figure 9a, b)*** and show three directional ranges: NE-SW (N050- N080), the most frequent, N090- N110 and N00- N10. Concerning general orientation according to the lineament length, the results highlight a cumulative length of 3.12.007 Km of lineaments ***(Figure 9c, d)***, and the directions with the longest lengths are: E-W-trending (N080- N110), the longest, then N050- N080; and N00- N10.

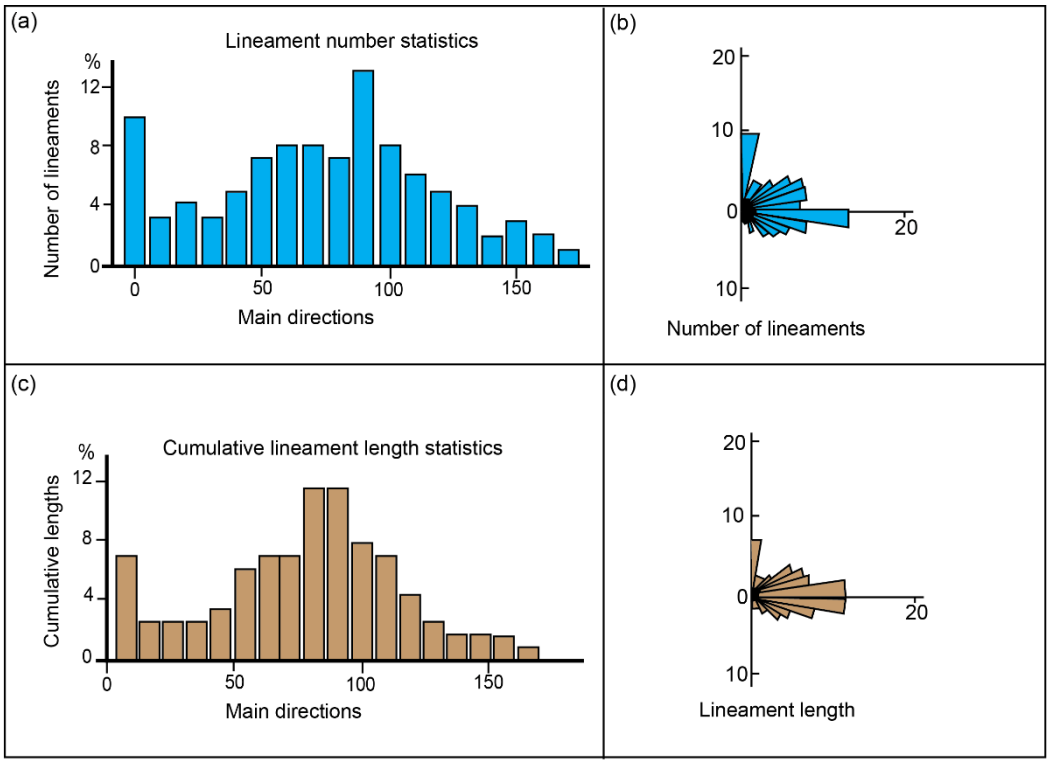

Figure 9 : *Statistical treatment of lineaments. a, b : depict the directional distribution of lineaments with respect to number. c, d : show the directional distribution of lineaments by length*

3-3-3. Correlation and spatial distribution of fractures per mesh

Statistical analysis reveals a good correlation between density in cumulative lengths and the number of lineaments, with a linear correlation coefficient of 0.806 ***(Figure 10)***. Therefore, the expression of fracturing intensity can be expressed in terms of either number or length. Nevertheless, to assess the homogeneity of fracturing over the study area, the prospect was divided into 35 meshes of 9 km². The rosettes of the main directions of each mesh show that the lineaments are distributed differently across the prospect ***(Figure 11)***.

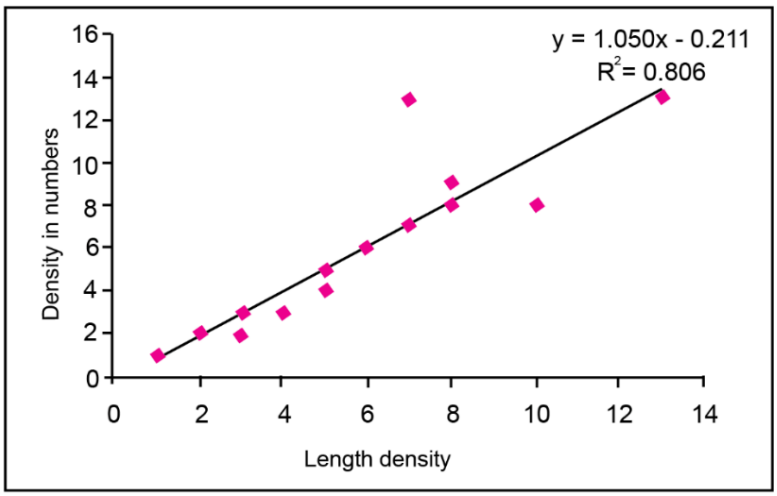

Figure 10 : *Relationship between density in length and number of lineaments*

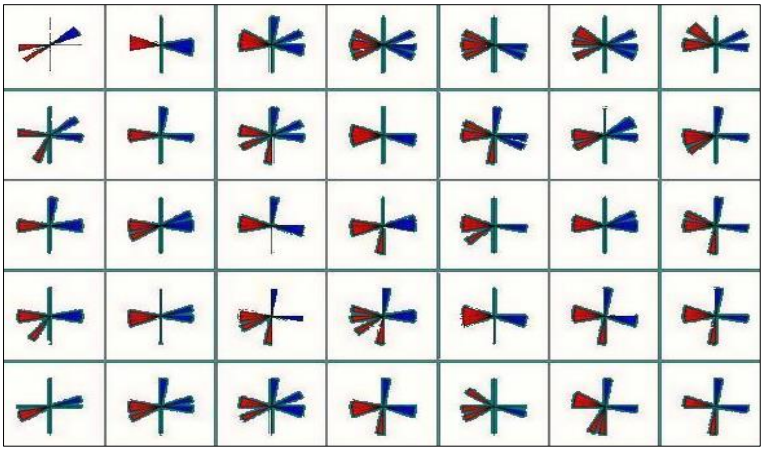

Figure 11 : *Major fracturing directions in 9 km² grids (threshold : 10 %)*

3-3-4. Fractures density

Low, medium and high-density zones can be identified, reflecting the heterogeneity of fracturing throughout the area. The distribution of fracture densities has enabled us to draw isovalue lines valid both as a function of fracture density linked to either number or cumulative length ***(Figure 12)***. Analysis of these maps reveals that fracture densities are particularly high in the central and northeastern parts, and are broadly trending NE-SW.

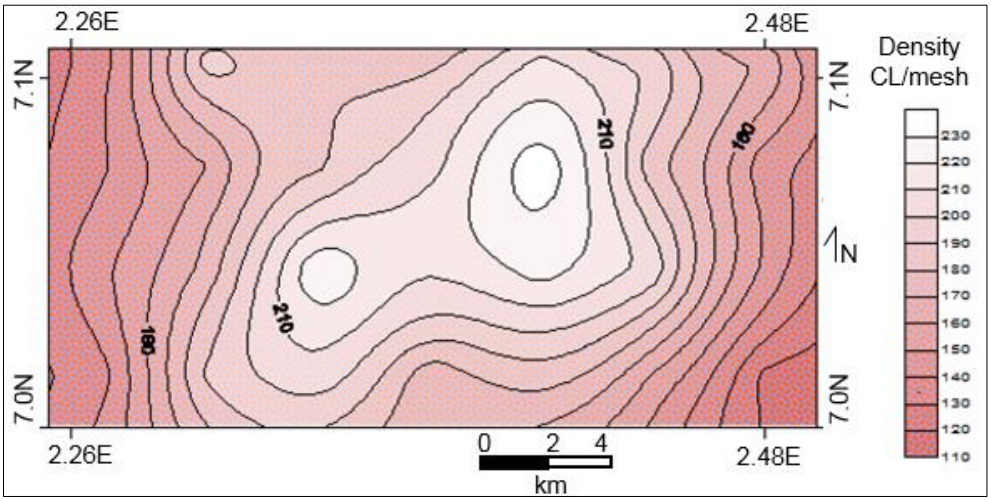

Figure 12 : *Fracture density map expressed in cumulative fracture length*

3-4. Relationship between lineament density and geochemical gold anomaly

We confronted the lineament intensity maps with the soil geochemistry map carried out in the area. The results reveal that the highest geochemical grades are located in the lineament anomaly, especially in the central part of the area. These anomalies are generally oriented NE-SW, so there may be a relationship between fracturing and gold mineralization ***(Figure 13)***. This therefore enables us to pinpoint interesting zones for future exploration drilling.

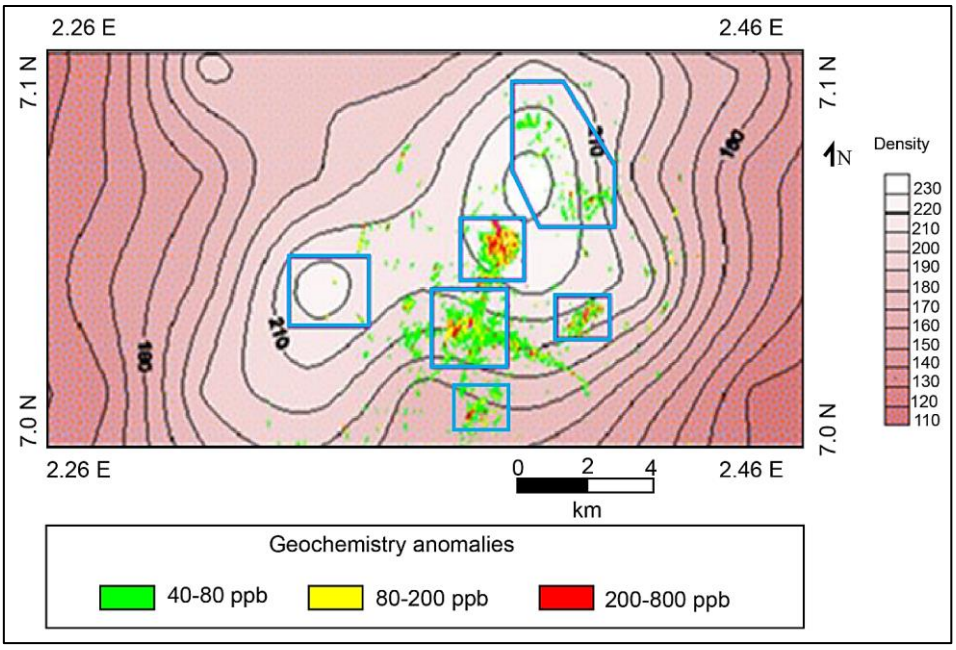

Figure 13 : *Map showing the overlapping of geochemical and lineament anomalies*

4. Discussion

4-1. Petrography features

The petrography of the study area is governed by metamorphic rocks, i.e. schists that are very frequently silicified, and volcanic rocks like basalt. The most prevalent formations are volcanic and schistose, metamorphosed under greenschist facies conditions. These metamorphic conditions are reminiscent of those observed by some authors on west African birimian trenches [26, 27]. A handful of plutonic formations were also observed, namely quartz gabbros at depth and pyrite granites. The latter are one of the few outcrops to be found in the study area. These findings are in line with those obtained in the region [22]. The mineralized zones in the region generally have a lithology consisting of volcanic formations including andesites, basalts and volcanosedimentary rocks [28]. The basalts and most of these rocks are thought to have formed in the Lower Birimian (between 2.2 and 2.15 Ga) [29, 30]. The observed lithologies show that the lithostratigraphy of this part of the trench is similar to that of most of the trenches in the Baoulé-Mossi domain [31, 32]. The lithology of our study area is very similar to that of Agbaou, but differs in the lack of granodiorite [26].

4-2. Deformation and structural features

Most of observed outcrops and deposits in the region are marked by fractures, shears and folds. We note the presence of structures characteristic of brittle deformation are abundant in the form of quartz veins and veinlets, faults, fracture schistosities and field joints. There are also structures characteristic of ductile deformation in the form of sigmoidal fissures, boudins and folds found on shales. Two shear directions were identified : a sinister direction between N010 and N025 and a dexter direction between N115 and N120. Statistical analysis of the fracture field, derived from satellite image processing, reveals a perfect correlation between cumulative lengths and the number of fractures. The N00-N010 and N090-N100 classes are the most prominent directions, followed by the secondary NE-SW (N040-N080) class. These directions have been identified in the Taabo area in the granitoids [33], and within Brobo region [34]. The NE-SW-trending faults are often dextral and are responsible for the thinning of the Fettékro Trench in the south and its flexion in the

north [34]. The high lineament density and large number of quartz veins and veinlets of varying trend recorded in the field reveal intense fracturing of the zone. These structures and their orientation have been recorded in other birimian trenches [22]. Indeed, the geological formations of the region underwent substantial fracturing during various tectonic events, notably during the Eburnian [34]. These fractures were discovered in the field and by remote sensing to confirm the lineament map on the one hand, and to define the major fractures on the other. As a consequence, the prevailing fracture direction is NE-SW, while the longer fractures are E-W. It is also noteworthy that N-S directions are very common in the Ivorian landscape, and are responsible for the drainage of numerous watercourses [25]. Outcrops and core samples have shown the slightest hint of sinister movement. This is an important fact in the context of mining exploration. In fact, these specific structures are good search clues, as they represent zones of weakness of particular significance in the development of deposits [35]. With respect to the results obtained on a scale model [36], the occurrence of echelon and sigmoid cracks helps to define the direction of shear movement, as well as the nature and direction of the stresses exerted [37]. Given that the maximum stress makes an angle of 45° with the shear direction, we can assume that the region underwent two compressive movements, one in the direction N055-N070 at the origin of the N010- N025 sinister shear and the other in the direction N155-N165 at the origin of the N110-120 dexter shear. This NW-SE compression and the various deformation phases that accompany it have also been reported in Burkina Faso [38], Côte d'Ivoire [39] and Ghana [40]. It is consistent with a second phase of deformation that involves progressive deformation linked to NW-SE regional compression, generating folds, thrusts and oblique shear zones, as described in Ghana [41]. Structural studies provide evidence for the existence of a shear zone. These features include sigmoidal structures typified by sigmoidal splits; shear joints or veins; boudins; shear-schistosity (C/S) plane associations; and asymmetrical folds [42].

4-3. Genetic character of gold deposit

Overall, the region's tectonics played a prominent role in setting up the mineralization, preparing the area for the ascent and subsequent circulation of mineralizing fluids in the fractures [43]. The study area was affected by intense fracturing forming a network of centimeter-scale stockworks in a shear zone within green and schistose rocks. Most mineralized zones occur within, or are spatially associated with shear zones, especially shear zones in larger systems of intersecting shear zone sets [44]. They range in shape from tabular to linear, and in form from disseminated, to breccia, to stockwork or sheeted veinlet zones, to single veins. Indeed, during phases of deformation, open fractures are created by N010-N025 sinister and N110-N120 dexter shearing. The relationship between the highest geochemical, lineament anomalies and shear deformation is consistent with the observation that the position of deposits in volcanic and volcano-sedimentary systems is always controlled by the network of faults that act as pathways for mineralizing fluids [45]. These fluids are at the root of the alterations observed in mineralized zones: silicification, sericitation, chloritization and pyritization. It is suggested that high fluid pressure gradients were set up at each crack-seal cycle, leading to a substantial increase in permeability and a significant concentration of fluid flow throughout the confined foliated zones [46]. This structure-induced infiltration mechanism allows the ore fluid to penetrate the deformation zones and also influences the deformation process by shifting the dissolved mineral components from the highly strained contacts to the deposition sites. In places, granitization appears to predate tectonics and is marked by contact metamorphism, while the rest of the study area is overlain by greenschist-type metamorphism. Based on this evidence, we can assert that the study area is classified as a shear-hosted gold deposit. Shear zones are a very important class of deposit, as they yield a large portion of the gold [47]. These deposits are most often found at the junction of ductile and brittle domains. They often form the secondary structures of major accidents, frequently at the edge of lithotectonic units. This class is very widespread in the West African Birimian [48,49]. Indeed, the mineralization of numerous Ivorian deposits such as Agbaou [50], Aféma [51] and Bonikro [52] is controlled by shear zones.

5. Conclusion

A petrographic study of the formations in the study area revealed three main lithological groups: plutonic formations such as granites, volcano-sedimentary groups consisting of seritoschists and chloritoschists, and volcanic formations including basalt and andesite. These formations have been affected by greenschist facies metamorphism and intense hydrothermal alteration characterized by silicification, sericitation, chloritisation and pyritisation. Lineament analysis revealed that the area was intensely fractured, with a roughly elongated anomaly running in the direction of the Birimian formations and strongly clustered in the central and north-eastern zones of the study area. Two shear corridors were identified: a sinister trending N010-N025 and a dexter shear trending N115-N120, which shape the current architecture of the area's geological formations, typified by rugged fissures, tight northeast-trending folds and quartz veins, classifying the study area among the shear-hosted gold deposit zone in the western Africa birimian.

References

[1] - S. MARVEL, Mineral Exploration Techniques : A Journey Beneath the Earth's Surface, https://medium.com/@StockMarvel/mineral-exploration-techniques-a-journey-beneath-the earths-surface-d98ded364921 (08 Avril 2024)

[2] - N. C. WHITE, Mining geology/Exploration, *Encyclopedia of Geology*, (2005) 613 - 623

[3] - A. I. AHMED, R. G. BRYANT and D. P. EDWARDS, Where are mines located in sub-Saharan Africa and how have they expanded overtime? *Land Degradation & Development*, 32 (1) (2020) 112 - 122

[4] - J. AMINOV, C. XI, B. ANMING, Y. MAMADJANOV and L. TUERHANJIANG, Comparison of multi-resolution optical Landsat-8, Sentinel-2 and Radar Sentinel-1 data for automatic lineament extraction : A case study of Alichur area, SE Pamir, Remote Sensing, (2019) 11778

[5] - E. D. EBONG, A. A. ABONG, E. B. ULEM and L. A. EBONG, Geoelectrical resistivity and geological characterization of hydrostructures for groundwater resource appraisal in the Obudu Plateau, Southeastern Nigeria, *Natural Resources Research*, 30 (2021) 2103 - 2117

[6] - S. DAS, S. D. PARDESHI, P. P. KULKARNI and A. DOKE, Extraction of lineaments from different azimuth angles using geospatial techniques: A case study of Pravara basin, Maharashtra, India", *Arab J Geosci,* 11 (2018) 160

[7] - U. C. NUGROHO and A. TJAHJANINGSIH, Lineament density information extraction using dem srtm data to predict the mineral potential zones, Vol. 13, N° 1 (2016) 67 - 74

[8] - I. A. EL-MAGD, H. MOHY and F. BASTA, "Application of remote sensing for gold exploration in the Fawakhir area, Central Eastern Desert of Egypt", *Arabian Journal of Geosciences*, 8 (2015) 3523 - 3536

[9] - A. B. POUR, B. ZOHEIR, B. PRADHAN and M. HASHIM, Multispectral and Hyperspectral Remote Sensing Data for Mineral Exploration and Environmental Monitoring of Mined Areas. *Remote Sens*, 13 - 3 (2021) 6 p.

[10] - S. N. GOWARD, J. MASEK, D. L. WILLIAMS, J. R. IRONS and R. J. THOMPSON, The Landsat 7 mission : Terrestrial research and applications for the 21st century, *Remote Sensing of Environment*, 78 (2001) 3 - 12

[11] - S. CASEMENT and L. WICKERT, Improvements in Mineralogical Classification with Increased Spectral Resolution: A Case Study over Cuprite, Nevada comparing Fused Bare Earth Composite and EnMAP Data, Mining, Science & Technology, https://blog.descarteslabs.com/improvements-mineralogical-classification-comparing-fused-bare-earth-composite-enmap-data (13 Avril 2024)

[12] - D. GABOURY, Ressources Mines et Industrie : Les minéralisations aurifères d'Afrique de l'Ouest : différences et similitudes avec l'Abitibi, *Ressources Mines et Industrie*, Vol. 6, N° 2 (2016) 37 - 42

[13] - Y. COULIBALY, B. KOUAHO, A. GNANZOU, M. E. ALLIALY and S. C. DJRO, Contexte geologique de la mineralisation aurifere du prospect de Bobosso (region de Dabakala, centre-nord de la Cote d'Ivoire), *Journal de la Recherche Scientifique de l'Université de Lomé*, Vol. 14, N° 2 (2012) 34 - 42

[14] - D. GORDON, Endeavour Mining Corporation, Lafigué Gold Project for the Fetekro Property Pre-Feasibility Study National Instrument, Technical Report, 2167-GREP-002, (2021) 43 - 101

[15] - Y. COULIBALY, M. C. BOIRON, M. CATHELINEAU and A. N. KOUAMELAN, Fluid immiscibility and gold deposition in the Birimian quartz veins of the Angovia deposit (Yaouré, Ivory Coast), *Journal of African Earth Sciences*, 50 (2008) 234 - 258

[16] - Z. OUATTARA and Y. COULIBALY, Pétrographie du gisement d'or de Bonikro, Sillon Birimien d'oume - Fettekro, Cote D'ivoire, *European Scientific Journal*, Vol. 11, N°21 (2015) 119 - 132

[17] - EQUIGOLD CI-SA, Rapport de prospection minière du permis d'Oumé (PR105), (2006) 11 p.

[18] - E. EGAL, C. CASTAING, P. CHEVREMENT, M. DONZEAU, C. GUERROT, S. KOTE, I. OUEDRAOGO, N. KAGAMBEGA, J. LE-METOUR, M. TEGYEY and D. THIEBLEMENT, Géological and structural framework of the Paleoproterozoic basement in Burkina Faso: mapping and geochronological constraints 20th Colloq. *Afric. Geol.*, Orleans, Abstracts, 2 (2004) 181 - 182

[19] - R. CABY, C. DELOR and O, AGOH, Lithologie, structure et métamorphisme des formations birimiennes dans la region d'Odiéné (Côte d'Ivoire) : rôle majeur du diapirisme des plutonset des décrochements en bordure du craton de Man, *J. Afr. Earth Sci*, 30 (2000) 351 - 374

[20] - R. LEPRETRE, Evolution phanérozoïque du Craton Ouest Africain et de ses bordures Nord et Ouest. Sciences de la Terre. Thèse de Doctorat, Université Paris Sud - Paris XI, (2015) 443 p.

[21] - K. B. K. POTHIN, P GIOAN et C. C. GRONAYES, Bilan géochronologique du socle précambrien de Côte d'Ivoire. Bio terre, *Rév. Inter. sci. De la vie et de la terre*, Vol. 1, N° 1 (2000) 36 - 47

[22] - M. B. SALEY, Système d'informations hydrogéologiques à référence spatiale, discontinuités pseudo-images et cartographies thématiques des ressources en eau de la région semi montagneuse de Man (Ouest de la côte d'ivoire). Thèse de doct. uni, Univ. Cocody, (2003) 209 p.

[23] - T. DUBE and O. MUTANGA, Evaluating the utility of the mediumspatial resolution Landsat-8 multispectral sensor in quantifying aboveground biomass in uMgeni catchment, South Africa, *Journal of Photogrammetry and Remote Sensing.*, 101 (2015) 36 - 46

[24] - H. S. PRASANTHA, Pre-processing of e0-1 hyperion data, *International journal of creative research thoughts*, 10 (6) (2022) f469 - f476

[25] - T. M. YOUAN, Apport de la télédétection à l'étude des aquifères de fissure du socle Précambrien d'Afrique de l'Ouest : analyse statistique et géostatistique des systèmes de fracture en imagerie Landsat 7 dans la région de Bondoukou (Est de la Côte d'Ivoire). Univ. Cocody-Abidjan, (2002) 97 p.

[26] - N. N. HOUSSOU, Etude pétrologique, structurale et métallogénique du gisement aurifère d'Agbahou, Divo, Côte d'Ivoire. Doctorat, Univ. Félix Houphouët -Boigny, (2013) 177 p.

[27] - F. BOURGES, P. DEBAT, F. TOLLON, M. MUNOZ and J. INGLES, The geology of the Taparko gold deposit, Birimiangreenstone belt, Burkina Faso, West Africa. *Mineralium Deposita*, 33 (1998) 591 - 605

[28] - Z. OUATTARA, Y. COULIBALY and F. LIEBEN, Petrographie du gisement d'or de Bonikro, sillon birimien d'Oume -Fettekro, Cote d'Ivoire, *European Scientific*, Vol. 11, N°2 (2015) 119 - 132

[29] - W. HIRDES and D. W. DAVIS, First U-Pb zircon age of extrusive volcanism in the Birimian Super group of Ghana/West Africa. *Journal of African Earth Sciences*, 27 (1998) 291 - 294

[30] - C. CASTAING, M. BILLA, J. P. MILESI, D. THIEBLEMONT, J. LE MENTOUR, E. EGAL, M. DONZEAU, C. GUERROT, A. COCHERIE, P. CHEVREMONT, M. TEGYEY, Y. ITARD, B. ZIDA, I. OUEDRAOGO et S. KOTE, Notice explicative de la carte géologique et miniére du Burkina Faso à 1/1 000 000. BRGM BUMIGEB, (2003) 147 p.

[31] - M. VIDAL, C. DELOR, A. POUCLET, Y. SIMEZON et G. AIRIC, Evolution géodynamique de l'Afrique de l'Ouest entre 2.2 et 2 Ga : style « Archéen » des ceintures vertes des ensembles sédimentaires birimiens du nord-est de la Côte d'Ivoire. Société Géologique de France, Vol. 167, N°3 (1996) 307 - 319

[32] - L. BARATOUX, V. METELKA, S. NABA, M. W. JESSELL, M. GREGOIRE and J. GANNE, Juvenile Juvenile Paleoproterozoic Crust Evolution during the Eburnean Orogeny (〜2.2-2.0 Ga), Western Burkina Faso. *Precambrian Research*, 191 (2011) 18 - 45

[33] - B. G. KOFFI et G. OUATTARA, Etude Pétrographique et Structurale des Granitoïdes du Site du Barrage de Taabo (Centre de la Côte d'Ivoire) : Contribution à la Compréhension des Pertes Possibles d'eau du Lac, *International Journal of Innovation and Applied Studies*, Vol. 2, N°4 (2013) 621 - 634

[34] - S. M. DAÏ BI, G. OUATTARA, G. B. KOFFI, A. GNANZOU et I. COULIBALY, Mise En Évidence de Nouvelles Structures Géologiques Dans La Région De Brobo (Centre De La Côte d'Ivoire). Aide À La Compréhension De La Tectonique Du Paléoprotérozoïque Du Craton Ouest Africain, *European Scientific Journal*, Vol. 14, N°18 (2018) 305 - 324

[35] - P. DEBAT, S. NIKIEMA, A. MERCIER, M. LOMPO, D. BEZIAT, F. BOURGES, M. RODDAZ, S. SALVI, F. TOLLON and U. WENMENGA, A new metamorphic constraint for the Eburnean orogeny from Palaeoproterozoic formations of the Man shield (Aribinda and Tampelga countries, Burkina Faso), *Precambrian Research*, 123, 1 (2003) 47 - 65 p.

[36] - G. L ROSENBAUM, G. S. ISTER and C. DUBOZ, Relative motions of Africa, Iberia and Europe during Alpine orogeny, *Tectonophysics*, 359 (2002) 117 - 29

[37] - N. MANDAL, Mode of development of sigmoidal en echelon fractures, *Earth Planet*, Vol. 104, N° 3 (1995) 453 - 464

[38] - A. OUÉDRAOGO, O. BAMBA, G. OUATTARA, E. GAMPINE and S. SAWADOGO, Caractérisations structurales des gîtes aurifères du corridor de Bouboulou-Bouda au Burkina Faso, Afrique de l'Ouest, *Afrique SCIENCE*, 12 (5) (2016) 89 - 104

[39] - M. VIDAL, C. GUMIAUX, F. CAGNARD, A. POUCLET, G. OUATTARA and M. PICHON, Evolution of a Paleoproterozoic "weaktype" orogeny in the Wes t African Craton (Ivory Coast). *Tectonophysics*, 477 (2009) 145 - 159

[40] - J. L. FEYBESSE, M. BILLA, C. GUERROT, E. DUGUEY and V. BOUCHOT, The paleoproterozoic Ghanaian province : Geodynamic model and ore controls, including regional stress modeling Research, *Precambrian Research*, 149, 3-4 (2006) 149 - 196

[41] - S. DAMPARE, T. SHIBATA, D. ASIEDU, O. OKANO, J. MANU and P. SAKYI, Sr–Nd isotopic compositions of Paleoproterozoic metavolcanic rocks from the southern Ashanti volcanic belt, Ghana. Okayama University, *Earth Science Reports*, 16, 1 (2009) 9 - 28

[42] - W. PASSCHIER and R. A. J. TROUW, Microtectonic. Éditions Springer, Berlin Heidelberg New York, (1998) 289 p.

[43] - C. CHANG, K. XIAO and G. LUO, Influence de différents paramètres tectoniques sur la formation de fractures et l'écoulement des fluides autour de l'intrusion magmatique de la croûte supérieure : aperçus de la modélisation numérique, *Earth Sci News*, 17 (2024) 2233 - 2253

[44] - C. J. HODGSON, The structure of shear-related, vein-type gold deposits : *A review, Ore Geology Reviews*, Vol. 4, Issue 3 (1989) 231 - 273 p.

[45] - A. MASOUD and K. KOIKE, Auto-detection and integration of tectonically significant lineaments from SRTM DEM and Remotely-sensed Geophysical data", *J of Photogramm and Remote Sensing*, 66 (2011) 818 - 832

[46] - C. A. BOULTER, M. G. FOTIOS and G. N. PHILLIPS, The Golden Mile, Kalgoorlie; a giant gold deposit localized in ductile shear zones by structurally induced infiltration of an auriferous metamorphic fluid, *Economic Geology*, Vol. 82, (7) (1990) 1661 - 1678

[47] - L. GIAMBIAGI, P. P. ÁLVAREZ, C. CREIXELL, D. MARDONEZ, I. MURILLO, R. VELÁSQUEZ, A. LOSSADA, J. SURIANO, J. MESCUA and M. BARRIONUEVO, Cenozoic Shift From Compression to Strike-Slip Stress Regime in the High Andes at 30°S, During the Shallowing of the Slab: Implications for the El Indio/Tambo Mineral District, Tectonics, 36 (2017) 2714 - 2735

[48] - T. OBERTHÜR, T. WEISER, and J. A. AMANOR, Mineralogical setting and distribution of gold in quartz veins and sulphide ores of the Ashanti mine and other deposits in the Ashanti belt of Ghana : genetic implications, Mineralium Deposita, 32 (1997) 2 - 15

[49] - S. SALVI, P. O. AMPONSAH, L. SIEBENALLER, D. BÉZIAT, L. BARATOUX and M. JESSELL, Shear-related gold mineralization in northwest Ghana: the Julie deposit. *Ore Geol. Rev.*, 78 (2015) 712 - 717

[50] - N. N. HOUSSOU, M. E. ALLIALY, F. J. KOUADIO and A. GNANZOU, Structural controlof auriferous mineralisation in the Birimian : case of the Agbahou deposit in the region of Divo, Côte d'Ivoire, *International Journal of Geoscience*, 8 (2017) 189 - 204

[51] - K. E. ASSIE, Lode gold mineralization in the Paleoproterozoic (Birimian) volcano-sedimentary sequence of Afema gold district, southeastern Côte d'Ivoire. Thesis, Faculty of Energy and Economic Sciences. *Technical University of Clausthal*, Germany, (2008) 198 p.

[52] - Z. OUATTARA, Y. COULIBALY and M. C. BOIRON, Shear-hosted gold mineralization in the Oumé-Fettèkro greenstone belt, Côte d'Ivoire : the Bonikro deposit. The Geological Society, London, Special Publications, (2020) p. SP502-2019-103. 10.1144/SP502-2019-103. hal-03007908